

## TO THE EDITOR:

# Prognostic value and oncogenic landscape of *TP53* alterations in adult and pediatric T-ALL

Mathieu Simonin,<sup>1-3,\*</sup> Guillaume P. Andrieu,<sup>1,2,\*</sup> Rudy Birsens,<sup>4,5</sup> Marie Balsat,<sup>6</sup> Guillaume Hypolite,<sup>1,2</sup> Lucien Courtois,<sup>1,2</sup> Carlos Graux,<sup>7</sup> Nathalie Grardel,<sup>8,9</sup> Jean-Michel Cayuela,<sup>10</sup> Françoise Hugué,<sup>11</sup> Yves Chalandon,<sup>12,13</sup> Yannick Le Bris,<sup>14</sup> Elizabeth Macintyre,<sup>1,3</sup> Virginie Gandemer,<sup>15</sup> Arnaud Petit,<sup>3</sup> Philippe Rousselot,<sup>16,17</sup> André Baruchel,<sup>18</sup> Didier Bouscary,<sup>4,5</sup> Olivier Hermine,<sup>19</sup> Nicolas Boissel,<sup>20</sup> and Wahid Asnafi<sup>1,2</sup>

<sup>1</sup>Laboratory of Onco-Hematology, Assistance Publique-Hôpitaux de Paris, Hôpital Necker Enfants-Malades, Université de Paris Cité, Paris, France; <sup>2</sup>Institut Necker-Enfants Malades, INSERM U1151, Paris, France; <sup>3</sup>Department of Pediatric Hematology and Oncology, Assistance Publique-Hôpitaux de Paris, Armand Trousseau Hospital, Sorbonne Université, Paris, France; <sup>4</sup>Department of Hematology, Hôpital Cochin, Assistance Publique-Hôpitaux de Paris, Université de Paris Cité, Paris, France; <sup>5</sup>Institut Cochin, INSERM U1016, Paris, France; <sup>6</sup>Hospices Civils de Lyon, Service d'Hématologie Clinique, Centre Hospitalier Lyon-Sud, Pierre-Bénite, France; <sup>7</sup>CHU UCLouvain Namur-Godinne, service d'Hématologie, Yvoir, Belgium; <sup>8</sup>Laboratory of Hematology, CHRU Lille, Lille, France; <sup>9</sup>INSERM U1172, Lille, France; <sup>10</sup>Laboratory of Hematology and EA3518, Saint-Louis University Hospital, Université de Paris Cité, Paris, France; <sup>11</sup>Department of Hematology, CHRU-Institut Universitaire de Cancer Toulouse-Oncopole, Toulouse, France; <sup>12</sup>Division of Hematology, Department of Oncology, University Hospital of Geneva and Faculty of Medicine, University of Geneva, Geneva, Switzerland; <sup>13</sup>Swiss Group for Clinical Cancer Research, Bern, Switzerland; <sup>14</sup>Hematology Biology, Nantes University Hospital and Nantes-Angers Cancer and Immunology Research Center, Nantes, France; <sup>15</sup>Department of Pediatric Hematology and Oncology, University Hospital of Rennes, Rennes, France; <sup>16</sup>Department of Hematology, Centre Hospitalier de Versailles, Le Chesnay, France; <sup>17</sup>Université Paris-Saclay, Communauté Paris-Saclay, France; <sup>18</sup>Department of Pediatric Hematology and Immunology, Assistance Publique-Hôpitaux de Paris, Robert Debré Hospital, Université de Paris Cité, Paris, France; <sup>19</sup>Department of Hematology, INSERM U1163, IMAGINE Institute, Paris University, Necker Hospital, Paris, France; and <sup>20</sup>Université Paris Cité, Institut de Recherche Saint-Louis, URP-3518, Assistance Publique-Hôpitaux de Paris, Saint-Louis University Hospital, Paris, France

Among hematologic malignancies, T-cell acute lymphoblastic leukemia (T-ALL) represents a class of aggressive tumors with dismal clinical outcome in cases of relapsed or refractory disease. Although the intensification of multiagent chemotherapy protocols has dramatically improved prognosis, refractory and relapsed cases are clinically challenging because of limited therapeutic options.<sup>1,2</sup> p53 is a transcription factor and a master tumor suppressor gene frequently altered in cancer.<sup>3</sup> In contrast to carcinomas and other hematologic malignancies, *TP53* alterations (*TP53*<sup>Alt</sup>), encompassing mutations (*TP53*<sup>Mut</sup>), and/or pan-exon deletions (*TP53*<sup>Del</sup>) are remarkably rare at diagnosis in T-ALL, and their clinical implication remains elusive.<sup>4-6</sup> Critically, *TP53*<sup>Alt</sup> have been reported to be acquired in up to 20% of the relapsed T-ALL cases, where they convey a deleterious prognosis.<sup>7-9</sup> Here, we produce the first comprehensive analysis of *TP53*<sup>Alt</sup> and the associated oncogenetic landscape in an extensive cohort of 476 patients newly diagnosed with T-ALL.

We investigated the clinical characteristics of *TP53*<sup>Alt</sup> in 476 patients including 215 adults and 261 children. Adult patients were enrolled in the GRAALL-2003-2005 trial (GRAALL-2003, #NCT00222027; GRAALL-2005, #NCT00327678), and pediatric patients were enrolled in the FRALLE 2000 trial (supplemental Figure 1, available on the *Blood* website). Based on the DNA availability for molecular analysis, 215 adult patients out of 337 and 261 pediatric patients out of 427 were included in this study. No difference in clinical outcomes was observed between the included patients and the entire cohort (supplemental Figures 2 and 3; supplemental Table 1). Diagnostic peripheral blood or bone marrow samples were collected after informed consent was obtained, according to the Declaration of Helsinki. All samples contained ≥80% blasts, immunophenotypic of T-ALL samples, minimal residual disease (MRD)

assessment, and multiplex ligation-dependent probe amplification analysis (P383 T-ALL, MRC Holland) were performed as previously described.<sup>10-12</sup>

Genomic analysis was performed using pan-exon targeted next-generation sequencing of DNA extracted from diagnostic samples, and DNA libraries were prepared using the Nextera XT kit (Illumina) and sequenced on a MiSeq (Illumina). The next-generation sequencing panel included 63 genes known to be mutated in T-ALL (supplemental Table 2). Genetic lesion co-occurrences and mutual exclusions were computed using the DISCOVER R package. We performed a computational approach previously described for the detection of copy number variants from next-generation sequencing data,<sup>13,14</sup> including a systematic analysis of the depth of *TP53* gene coverage. This method is based on variations in the depth of coverage of the aligned sequence reads using a locally developed algorithm. The copy number variants detected were confirmed by high-resolution comparative genomic hybridization and/or multiplex ligation-dependent probe amplification analysis (kits P037-CLL-1 and P038-CLL-2, MRC Holland). Diagnostic DNA was hybridized on a Cytogenetics Whole-Genome 2.7M Array (Affymetrix, Santa Clara, CA) (comparative genomic hybridization array), according to the manufacturer's recommendations. Data analysis was performed using Chromosome Analysis Suite software (Affymetrix). Gene copy number aberrations were compared with the Database of Genomic Variants<sup>15</sup> to study only somatic aberrations.

Comparisons of categorical and continuous variables between subgroups were performed using Fisher exact test and the Mann-Whitney test, respectively. Overall survival (OS) was calculated from the date of diagnosis to the last follow-up date,

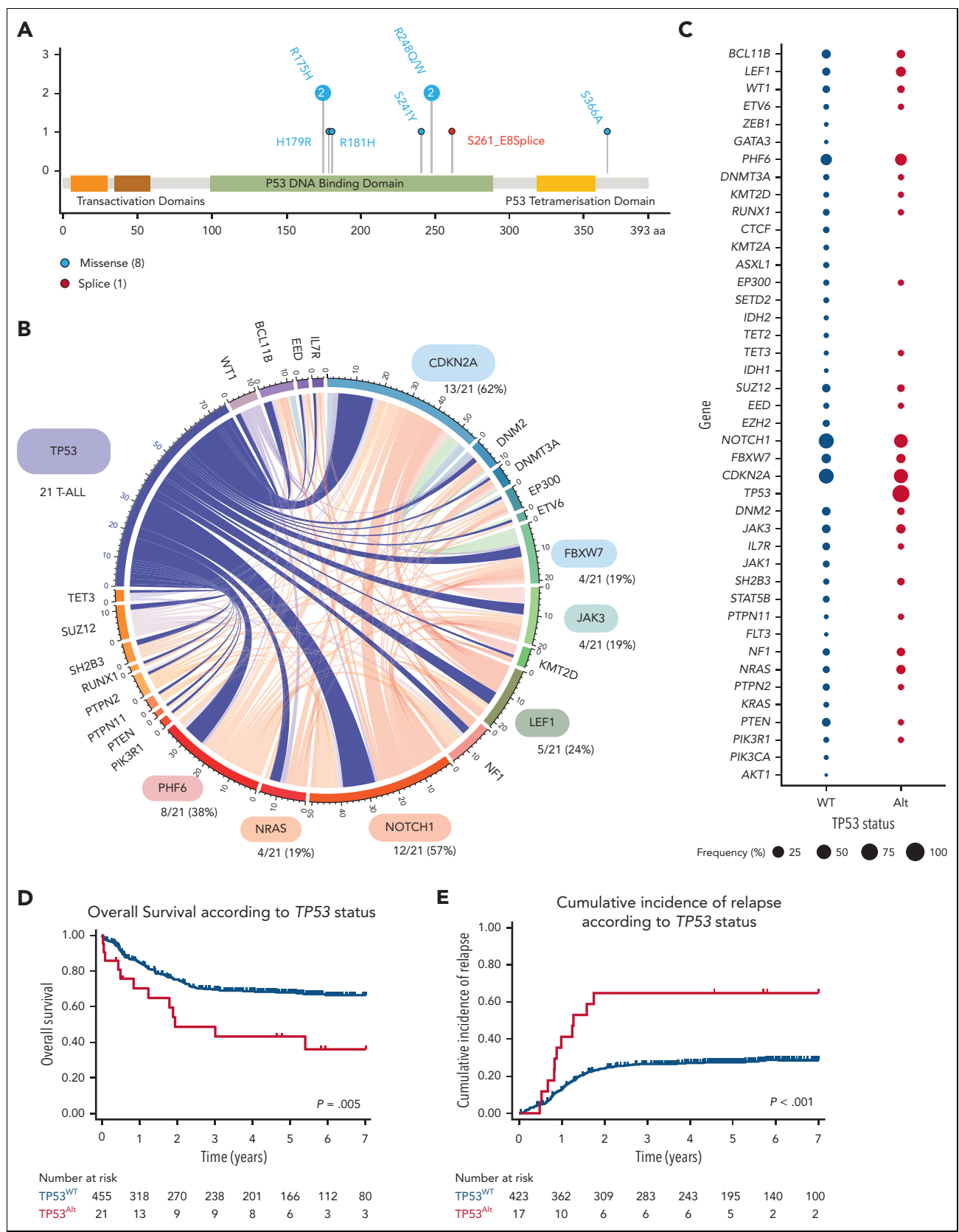


**Figure 1. TP53 alterations in the GRAALL03/05 and FRALLE2000 studies.** (A) Lollipop plots indicating  $TP53$  mutations in 476 patients with T-ALL. More details on the pathogenicity of the  $TP53$  mutations are provided in supplemental Table 4. (B) Circos plots illustrating pairwise relationships across relatively common mutated genes in  $TP53^{Alt}$  T-ALL. The width of the ribbon corresponds to the number of cases with the simultaneous presence of a first and second gene mutation. (C) Frequency of alterations per gene in  $TP53^{Alt}$  vs  $TP53^{WT}$  T-ALL. The width of the circles is proportional to the frequency of alterations observed in the 2 T-ALL subgroups ( $TP53^{Alt}$  in red vs  $TP53^{WT}$  T-ALL in blue). (D-E) Clinical impact of  $TP53^{Alt}$  in the GRAALL0305 and FRALLE2000 studies. OS (D) and CIR (E) are shown. The red curve represents patients with  $TP53^{Alt}$  T-ALL and the blue curve represents patients with  $TP53^{WT}$ .

**Table 1. Clinicobiological and outcome characteristics of adult and pediatric T-ALL (GRAALL and FRALLE protocols) according to TP53 status**

Variable	TP53 <sup>Alt</sup>	TP53 <sup>WT</sup>	Total	P value*		
	n = 21 (4%)	n = 455 (96%)	N = 476			
Male (%)	14/21 (67)	343/455 (75)	357/476 (75)	.4		
Age, y†	23.4 (4.0-51.8)	15.3 (1.1-59.1)	15.3 (1.1-59.1)	.5		
WBC, g/L‡	25 (5-674)	66 (0-980)	64 (0-980)	<b>.01</b>		
CNS involvement (%)‡	3/21 (14)	48/453 (11)	51/474 (11)	.5		
<b>Immunophenotype (%)</b>						
Early thymic precursor phenotype	6/16 (38)	50/291 (17)	56/307 (18)	.09		
Immature (IM0/δ/γ)§	8/20 (40)	81/399 (20)	89/419 (21)	<b>.048</b>		
αβ lineage	6/20 (30)	205/399 (51)	211/419 (50)	.07		
Mature TCRγδ	3/20 (15)	63/399 (16)	66/419 (16)	>.9		
<b>Oncogenetic classification (%)</b>						
TLX1	1/18 (6)	53/397 (13)	54/415 (13)	.5		
TLX3	2/18 (11)	70/397 (18)	72/415 (17)	.8		
SIL-TAL1	1/18 (6)	56/397 (14)	57/415 (14)	.5		
CALM-AF10	0/18 (0)	13/397 (3)	13/415 (3)	>.9		
High-risk classifier	13/21 (62)	196/455 (43)	209/476 (44)	.12		
<b>Treatment response (%)</b>						
Prednisone response	13/21 (62)	246/446 (55)	259/467 (55)	.7		
Chemosensitivity	12/21 (57)	325/446 (73)	337/467 (72)	.1		
MRD1 >10 <sup>-4</sup>	9/12 (75)	114/328 (35)	123/340 (36)	<b>.01</b>		
Complete remission	17/21 (81)	423/455 (93)	440/476 (92)	.07		
Allo-HSCT	4/20 (20)	97/436 (22)	101/456 (22)	.7		
<b>Outcome, %</b>						
5-y CIR (95% CI)	65 (11-43)	27 (23-32)	29 (25-33)	<b>&lt;.001</b>		
5-y OS (95% CI)	48 (26-67)	72 (68-76)	71 (67-75)	<b>.005</b>		
	<b>Univariate and multivariate analysis¶</b>					
	<b>Univariate</b>			<b>Multivariate</b>		
	<b>Specific HR</b>	<b>95% CI</b>	<b>P value</b>	<b>Specific HR</b>	<b>95% CI</b>	<b>P value</b>
<b>CIR</b>						
Age, y	1.01	0.98-1.03	.57	—	—	—
CNS	1.57	0.85-2.59	.08	1.28	0.77-2.13	.34
Log (WBC)	1.62	1.2-2.18	<b>.002</b>	1.62	1.19-2.19	<b>.002</b>
Prednisone response	0.67	0.47-0.95	<b>.03</b>	0.93	0.64-1.35	.70
High-risk classifier§	2.78	1.94-3.99	<b>&lt;.001</b>	2.58	1.78-3.74	<b>&lt;.001</b>
TP53 <sup>Alt</sup>	3.11	1.67-5.78	<b>&lt;.001</b>	2.90	1.55-5.44	<b>.001</b>

MRD1 correspond to MRD evaluation after induction and was performed by allele-specific oligonucleotides polymerase chain reaction. TCR status and oncogenic were performed as described in [supplemental Methods](#).

P < .05 are indicated in bold.

allo-HSCT, allogeneic hematopoietic stem cell transplantation; CNS, central nervous system; WBC, white blood count.

\*Statistical tests performed: Fisher exact test and Wilcoxon rank-sum test.

†Statistics presented: median (minimum-maximum).

‡CNS involvement: CNS3 in FRALLE2000 trial, CNS2 and/or CNS3 in GRAALL2003 and GRAALL2005 trial.

§T-ALL are divided into 3 subclasses as following: (1) immature (no detectable TCRβ variable diversity joining): IM0 (TCRδ and TCRγ germ line), IM6 (TCRδ rearranged but not TCRγ), and IM9 (both TCRδ and TCRγ rearranged); (2) T-ALL with TCRαβ lineage (including both early-cortical IMb/pre-αβ and mature sTCRαβ\*); and (3) mature sTCRγδ.<sup>12</sup>

||Low-risk classifier: NOTCH1 and/or FBXW7 (N/F) mutation without N/K-RAS and PTEN (R/P) alteration. High-risk classifier: N/F mutation with R/P alteration, N/F WT with or without R/P alteration.<sup>10,16</sup>

¶Univariate and multivariate Cox analyses stratified on protocol.

**Table 1 (continued)**

	Univariate and multivariate analysis†					
	Univariate			Multivariate		
	HR	95% CI	P value	HR	95% CI	P value
<b>OS</b>						
Age	1.03	1.01-1.05	<b>.001</b>	1.05	1.03-1.07	<b>&lt;.001</b>
CNS	2.00	1.28-3.14	<b>.002</b>	1.64	1.02-2.64	<b>.04</b>
Log (WBC)	1.99	1.48-2.67	<b>&lt;.001</b>	2.01	1.51-2.86	<b>&lt;.001</b>
Prednisone response	0.54	0.38-0.76	<b>&lt;.001</b>	0.83	0.57-1.20	.31
High-risk classifier	2.93	2.06-4.17	<b>&lt;.001</b>	2.90	2.01-4.18	<b>&lt;.001</b>
<i>TP53</i> <sup>Alt</sup>	2.34	1.30-4.24	<b>.005</b>	2.87	1.56-5.26	<b>.001</b>

MRD1 correspond to MRD evaluation after induction and was performed by allele-specific oligonucleotides polymerase chain reaction. TCR status and oncogenic were performed as described in supplemental Methods.

P < .05 are indicated in bold.

allo-HSCT, allogeneic hematopoietic stem cell transplantation; CNS, central nervous system; WBC, white blood count.

\*Statistical tests performed: Fisher exact test and Wilcoxon rank-sum test.

†Statistics presented: median (minimum-maximum).

‡CNS involvement: CNS3 in FRALLE2000 trial, CNS2 and/or CNS3 in GRAALL2003 and GRAALL2005 trial.

§T-ALL are divided into 3 subclasses as following: (1) immature (no detectable TCR $\beta$  variable diversity joining): IM0 (TCR $\delta$  and TCR $\gamma$  germ line), IM $\delta$  (TCR $\delta$  rearranged but not TCR $\gamma$ ), and IM $\gamma$  (both TCR $\delta$  and TCR $\gamma$  rearranged); (2) T-ALL with TCR $\alpha\beta$  lineage (including both early-cortical IMb/pre- $\alpha\beta$  and mature sTCR $\alpha\beta$ ); and (3) mature sTCR $\gamma\delta$ .<sup>12</sup>

|| Low-risk classifier: *NOTCH1* and/or *FBXW7* (N/F) mutation without *N/K-RAS* and *PTEN* (R/P) alteration. High-risk classifier: *N/F* mutation with *R/P* alteration, *N/F* WT with or without *R/P* alteration.<sup>10,16</sup>

¶Univariate and multivariate Cox analyses stratified on protocol.

censoring patients alive. The cumulative incidence of relapse (CIR) was calculated from the complete remission date to the date of relapse, and censoring patients alive without relapse at the last follow-up date. Relapse and death in complete remission were considered to be competitive events. Univariate and multivariate analyses to assess the impact of categorical and continuous variables were performed using the Cox model. The proportional-hazards assumption was checked before conducting the multivariate analyses. In the univariate and multivariate analyses, age and log<sub>10</sub> (white blood count) were considered continuous variables. All the analyses were stratified during the trial. Variables with *P* < .1 in univariate analysis were included in the multivariable models. Statistical analyses were performed using the STATA software (STATA 12.0 Corporation, College Station, TX). All *P* values were 2-sided, with *P* < .05 denoting statistical significance. Additional details are included in the supplemental Methods.

The incidence of *TP53*<sup>Alt</sup> at the time of diagnosis in this cohort was 4% (21/476). *TP53*<sup>Mut</sup> was detected in 9 patients (6 adults and 3 pediatric cases) (Figure 1A; supplemental Tables 3 and 4), *TP53*<sup>Del</sup> was identified in 15 patients (7 adult and 8 pediatric cases), and 3 patients harbored both *TP53*<sup>Mut</sup> and *TP53*<sup>Del</sup>. Patients with *TP53*<sup>Alt</sup> did not significantly differ from patients with *TP53* wild-type (*TP53*<sup>WT</sup>) regarding sex, age, and central nervous system involvement (Table 1), but were associated with an immature phenotype (combining IM0 T-ALL; T-cell receptor  $\delta$  [TCR $\delta$ ] and TCR $\gamma$  germ line, IM $\delta$  T-ALL; TCR $\delta$  rearranged but not TCR $\gamma$  and IM $\gamma$  T-ALL; both TCR $\delta$  and TCR $\gamma$  rearranged)<sup>12</sup> (8/20 [40%] vs 81/399 [20%], *P* = .048). The oncogenic landscape of *TP53*<sup>Alt</sup> was comparable to that of *TP53*<sup>WT</sup> T-ALLs (Figure 1B-C; supplemental Figures 4-6; supplemental Table 5). To investigate the prognostic value of *TP53*<sup>Alt</sup>, survival analyses

were performed on the series of 476 patients. *TP53*<sup>Alt</sup> did not confer an increased poor prednisone response, defined by a peripheral blood blast count >1.0 × 10<sup>9</sup>/L at the end of the induction phase (38% vs 45%, *P* = .7) (Table 1). Although *TP53*<sup>Alt</sup> did not significantly influence the morphological complete response rate at the end of the induction course (81% vs 93%, *P* = .07), patients harboring *TP53*<sup>Alt</sup> were associated with delayed early medullary blast clearance, as confirmed by the end of induction MRD1 assessment, with more positivity ( $\geq 10^{-4}$ ) in *TP53*<sup>Alt</sup> than in *TP53*<sup>WT</sup> cases (75% vs 35%, *P* = .01). Patients (both adult and pediatric) with *TP53*<sup>Alt</sup> had an inferior outcome compared with *TP53*<sup>WT</sup> (Table 1; Figures 1D-E; supplemental Figure 7), with an increased CIR (5-year CIR: 65% vs 27%; specific hazard ratio [HR], 3.1; 95% confidence interval [CI], 1.67-5.78; *P* < .001) and a shorter OS (5-year OS: 48% vs 72%; HR, 2.34; 95% CI, 1.30-4.24; *P* = .005). In multivariate analysis, *TP53*<sup>Alt</sup> predicted a statistically lower OS (HR, 2.87; 95% CI, 1.56-5.26; *P* = .001) and higher CIR (specific HR, 2.90; 95% CI, 1.55-5.44; *P* = .001) even after adjustment on the 4 genes *NOTCH1*/*FBXW7*/*RAS*/*PTEN* (*NFRP*) classifier, which identified patients with a poor prognosis in both GRAALL and FRALLE trials.<sup>10,16</sup>

The limited number of MRD1 assessments available for patients with *TP53*<sup>Alt</sup> T-ALL (12/21, 57%) did not allow us to include this end point in the multivariate analysis, justifying further studies to establish whether this alteration remains an independent prognostic factor when combined with MRD1 status in T-ALL.

This study provides the largest comprehensive analysis of *TP53*<sup>Alt</sup> in T-ALL, describing, for the first time, their clinical profile and, most importantly, the extremely poor prognostic impact associated with *TP53*<sup>Alt</sup> at diagnosis in T-ALL, urging the

need to develop innovative targeted therapies for patients harboring *TP53*<sup>Alt</sup>.

Approximately 25% of pediatric patients and 50% of adult patients with T-ALL relapse, with a 5-year survival rate of less than 20% in both age groups.<sup>1,2</sup> The sole therapeutic approaches with curative potential for T-ALL relapsed cases are limited to conventional chemotherapy or hematopoietic stem cell transplantation. Molecular genetic analyses and sequencing studies have recently led to the identification of recurrent T-ALL alterations associated with prognosis, allowing for the refinement of the stratification of relapse risk.<sup>10,14,17,18</sup> However, a significant proportion of T-ALL relapses remain unpredicted, underlining the need for new predictive markers.

Negative outcomes observed in *TP53*<sup>Alt</sup> T-ALL are likely to be related to p53-induced therapeutic resistance previously described for other malignancies, combined with loss of p53 tumor suppressor activity and acquisition of novel functions that disrupt the DNA damage response pathway.<sup>19,20</sup> APR-246 (eprenetapopt), a small molecule interacting with mutated p53 protein to restore its WT conformation,<sup>21,22</sup> has recently shown promising results in myeloid malignancies and B-cell ALL,<sup>23-26</sup> justifying further studies to explore the potential efficacy of this new drug in T-ALL *TP53*<sup>Mut</sup>.

## Acknowledgments

The authors thank all the participants of the GRAALL-2003 and GRAALL-2005 study groups, the Société Française de Lutte contre les Cancers et les leucémies de l'Enfant et de l'adolescent (SFCE) and the investigators of the 16 SFCE centers involved in the collection and provision of data and patient samples, and V. Lheritier for the collection of clinical data.

This study was supported by grants to Necker laboratory from the Cancer Research for Personalized Medicine (CARPEM), the Association pour la Recherche contre le Cancer (Equipe Labellisée), the Ligue contre le Cancer (Equipe Labellisée), and the Institut National du Cancer PRT-K 18-071. The GRAALL study was supported by grants from the Programme Hospitalier de Recherche Clinique (grants P0200701 and P030425/AOM03081), Ministère de l'Emploi et de la Solidarité, France, and the Swiss Federal Government in Switzerland. Samples were collected and processed by the Assistance Publique-Hôpitaux de Paris "Direction de Recherche Clinique" Tumor Bank at Necker-Enfants Malades. M.S. was supported by Action Leucémie, la Ligue contre le Cancer et Soutien pour la formation à la recherche translationnelle en cancérologie. G.P.A. was supported by the Fondation de France.

## Authorship

Contribution: V.A., O.H., M.S., and G.P.A. conceived and designed the research and oversaw the project; M.B., C.G., N.G., J.-M.C., F.H., Y.C., Y.L.B., E.M., V.G., A.P., P.R., A.B., D.B., O.H., N.B., and V.A. provided study materials or patients; M.S., G.P.A., G.H., L.C., and V.A. performed molecular analyses; M.S. and G.P.A. collected and assembled data; N.B. and M.S. performed statistical analysis; M.S., G.P.A., R.B., O.H., V.A., and N.B. analyzed and interpreted data; and M.S., G.P.A., N.B., and V.A. wrote the manuscript.

Conflict-of-interest disclosure: The authors declare no competing financial interests

ORCID profiles: M.S., 0000-0002-0448-8811; G.P.A., 0000-0003-0289-4952; N.G., 0000-0001-6573-1312; F.H., 0000-0002-9576-8578; Y.C., 0000-0001-9341-8104; Y.L.B., 0000-0002-0095-6999; E.M., 0000-0003-0520-0493; V.G., 0000-0002-4991-233X; A.P., 0000-0001-8363-1622; P.R., 0000-0003-3238-4494; N.B., 0000-0003-2091-7927.

Correspondence: Vahid Asnafi, Laboratory of Onco-Hematology, Assistance Publique-Hôpitaux de Paris (APHP), Necker Enfants-Malades Hospital, Université de Paris, 149 rue de Sèvres, 75015 Paris, France; email: vahid.asnafi@aphp.fr.

## Footnotes

Submitted 13 July 2022; accepted 21 December 2022; prepublished online on *Blood* First Edition 4 January 2023.

\*M.S. and G.P.A. contributed equally to this work and are joint first authors.

Data are available on request from the corresponding author, Vahid Asnafi (vahid.asnafi@aphp.fr).

The online version of this article contains a data supplement.

## REFERENCES

- Desjonquères A, Chevallier P, Thomas X, et al. Acute lymphoblastic leukemia relapsing after first-line pediatric-inspired therapy: a retrospective GRAALL study. *Blood Cancer J*. 2016;6(12):e504-510.
- Bhojwani D, Pui C-H. Relapsed childhood acute lymphoblastic leukaemia. *Lancet Oncol*. 2013;14(6):e205-217.
- Levine AJ. p53: 800 million years of evolution and 40 years of discovery. *Nat Rev Cancer*. 2020;20(8):471-480.
- Kawamura M, Ohnishi H, Guo SX, et al. Alterations of the p53, p21, p16, p15 and RAS genes in childhood T-cell acute lymphoblastic leukemia. *Leuk Res*. 1999;23(2):115-126.
- Van Vlierbergh P, Ambesi-Impiombato A, De Keersmaecker K, et al. Prognostic relevance of integrated genetic profiling in adult T-cell acute lymphoblastic leukemia. *Blood*. 2013;122(1):74-82.
- Stengel A, Schnitter S, Weissmann S, et al. TP53 mutations occur in 15.7% of ALL and are associated with MYC-rearrangement, low hypodiploidy, and a poor prognosis. *Blood*. 2014;124(2):251-258.
- Richter-Pechańska P, Kunz JB, Hof J, et al. Identification of a genetically defined ultra-high-risk group in relapsed pediatric T-lymphoblastic leukemia. *Blood Cancer J*. 2017;7(2):e523-531.
- Hof J, Kox C, Groeneveld-Krentz S, et al. NOTCH1 mutation, TP53 alteration and myeloid antigen expression predict outcome heterogeneity in children with first relapse of T-cell acute lymphoblastic leukemia. *Haematologica*. 2017;102(7):e249-e252.
- Diccianni MB, Yu J, Hsiao M, et al. Clinical significance of p53 mutations in relapsed T-cell acute lymphoblastic leukemia. *Blood*. 1994;84(9):3105-3112.
- Trinquand A, Tanguy-Schmidt A, Ben Abdelali R, et al. Toward a NOTCH1/FBXW7/RAS/PTEN-based oncogenetic risk classification of adult T-cell acute lymphoblastic leukemia: a Group for Research in Adult Acute Lymphoblastic Leukemia study. *J Clin Oncol*. 2013;31(34):4333-4342.
- Bond J, Marchand T, Touzart A, et al. An early thymic precursor phenotype predicts outcome exclusively in HOXA-overexpressing adult T-cell acute lymphoblastic leukemia: a Group for Research in Adult Acute Lymphoblastic Leukemia study. *Haematologica*. 2016;101(6):732-740.
- Asnafi V, Beldjord K, Boulanger E, et al. Analysis of TCR, pT alpha, and RAG-1 in T-acute lymphoblastic leukemias improves understanding of early human T-lymphoid lineage commitment. *Blood*. 2003;101(7):2693-2703.
- Yoon S, Xuan Z, Makarov V, Ye K, Sebat J. Sensitive and accurate detection of copy number variants using read depth of coverage. *Genome Res*. 2009;19(9):1586-1592.
- Simonin M, Lhermitte L, Dourthe M-E, et al. IKZF1 alterations predict poor prognosis in adult and pediatric T-ALL. *Blood*. 2021;137(12):1690-1694.

15. MacDonald JR, Ziman R, Yuen RK, Feuk L, Scherer SW. The Database of Genomic Variants: a curated collection of structural variation in the human genome. *Nucleic Acids Res.* 2014;42(Database issue):D986-D992.
  16. Petit A, Trinquand A, Chevret S, et al. Oncogenetic mutations combined with MRD improve outcome prediction in pediatric T-cell acute lymphoblastic leukemia. *Blood.* 2018;131(3):289-300.
  17. Bond J, Touzart A, Leprêtre S, et al. DNMT3A mutation is associated with increased age and adverse outcome in adult T-cell acute lymphoblastic leukemia. *Haematologica.* 2019;104(8):1617-1625.
  18. Simonin M, Schmidt A, Bontoux C, et al. Oncogenetic landscape and clinical impact of IDH1 and IDH2 mutations in T-ALL. *J Hematol Oncol.* 2021;14(1):74-80.
  19. Hientz K, Mohr A, Bhakta-Guha D, Efferth T. The role of p53 in cancer drug resistance and targeted chemotherapy. *Oncotarget.* 2016;8(5):8921-8946.
  20. Mantovani F, Collavin L, Del Sal G. Mutant p53 as a guardian of the cancer cell. *Cell Death Differ.* 2019;26(2):199-212.
  21. Lambert JMR, Gorzov P, Vepritssev DB, et al. PRIMA-1 reactivates mutant p53 by covalent binding to the core domain. *Cancer Cell.* 2009;15(5):376-388.
  22. Bykov VJN, Issaeva N, Shilov A, et al. Restoration of the tumor suppressor function to mutant p53 by a low-molecular-weight compound. *Nat Med.* 2002;8(3):282-288.
  23. Cluzeau T, Sebert M, Rahmé R, et al. Eprenetapopt plus azacitidine in TP53-mutated myelodysplastic syndromes and acute myeloid leukemia: a phase II study by the Groupe Francophone des Myélodysplasies (GFM). *J Clin Oncol.* 2021;39(14):1575-1583.
  24. Demir S, Boldrin E, Sun Q, et al. Therapeutic targeting of mutant p53 in pediatric acute lymphoblastic leukemia. *Haematologica.* 2020;105(1):170-181.
  25. Sallman DA, DeZern AE, Garcia-Manero G, et al. Eprenetapopt (APR-246) and azacitidine in TP53-mutant myelodysplastic syndromes. *J Clin Oncol.* 2021;39(14):1584-1594.
  26. Mishra A, Tamari R, DeZern AE, et al. Eprenetapopt plus azacitidine after allogeneic hematopoietic stem-cell transplantation for TP53-mutant acute myeloid leukemia and myelodysplastic syndromes. *J Clin Oncol.* 2022;40(34):3985-3993.
- <https://doi.org/10.1182/blood.2022017755>
- © 2023 by The American Society of Hematology

## TO THE EDITOR:

# Diffuse myocardial fibrosis occurs in young patients with sickle cell anemia despite early disease-modifying therapy

Cara E. Morin,<sup>1,2,\*</sup> Akshay Sharma,<sup>3,\*</sup> Subodh Selukar,<sup>4</sup> Gary Beasley,<sup>5</sup> Anthony Merlocco,<sup>2,5,6</sup> Chris Goode,<sup>2</sup> Parul Rai,<sup>7</sup> Jeffrey A. Towbin,<sup>5</sup> Jane S. Hankins,<sup>7,†</sup> and Jason N. Johnson<sup>2,5,6,†</sup>

<sup>1</sup>Department of Radiology, Cincinnati Children's Hospital Medical Center, Cincinnati, OH; <sup>2</sup>Department of Diagnostic Imaging, <sup>3</sup>Department of Bone Marrow Transplantation and Cellular Therapy, and <sup>4</sup>Department of Biostatistics, St. Jude Children's Research Hospital, Memphis, TN; <sup>5</sup>Division of Pediatric Cardiology and <sup>6</sup>Division of Pediatric Radiology, University of Tennessee Health Science Center, Le Bonheur Children's Hospital, Memphis, TN; and <sup>7</sup>Department of Hematology, St. Jude Children's Research Hospital, Memphis, TN

We read with great interest the recent report from Niss et al.<sup>1</sup> Our group has recently reviewed data from a similar population at our institution, which does not support the conclusion of Niss et al that diffuse myocardial fibrosis is prevented by early initiation of disease-modifying therapy (DMT).

Cardiovascular complications are the leading cause of early mortality in patients with sickle cell anemia (SCA).<sup>2</sup> Yet, the pathobiology of sickle cell cardiomyopathy is incompletely understood and likely multifactorial.<sup>3</sup> Chronic anemia leads to global cardiac enlargement and myocardial hypertrophy. Global cardiac chamber dilation is a common feature in patients with SCA, and enlarged left atrial (LA) volume is a marker of diastolic dysfunction in SCA.<sup>4</sup> Repetitive microvascular ischemic insults and associated reperfusion injury may contribute to diffuse myocardial fibrosis and myocardial remodeling in individuals with SCA.<sup>5-7</sup>

Cardiovascular magnetic resonance (CMR) imaging is the only noninvasive method capable of accurately and reproducibly assessing heart size and function as well as characterizing the myocardium. Emerging data suggest that patients with SCA develop diffuse myocardial fibrosis,<sup>1,5-7</sup> detected by quantifying

the myocardial extracellular volume (ECV). Increased ECV fraction correlates strongly with histologically quantified myocardial fibrosis.<sup>8</sup> Our goal was to estimate the prevalence of diffuse myocardial fibrosis in a cohort of young individuals with SCA.

At our institution, all patients with SCA undergo cardiac surveillance starting at 16 years of age, which comprises a clinical assessment by a cardiologist and an echocardiogram. The presence of LA dilation (LA volume > 34 mL/m<sup>2</sup>), left ventricular dilation, or prominent trabeculations seen by echocardiogram led to patients being referred for CMR (detailed echocardiographic data in supplemental Table 1, on the *Blood* website). We performed a retrospective chart review of pediatric and young adult patients with SCA who underwent CMR at our institution between 2020 and 2021. Demographic and clinical information was obtained from reviewing the electronic medical record. A waiver of the requirement for informed consent was granted by the institutional review board for use of deidentified data.

CMR was performed on a 1.5T scanner (Avanto Fit; Siemens Medical Solutions, Inc, Erlangen, Germany). The protocol